An investigation on the effects of feature size in ultrasonic vibration-assisted sculpturing of microlens array

Canbin Zhang[1,#], Chi Fai Cheung[1], Xiaoliang Liang[1] and Benjamin Bulla[2]

1 State Key Laboratory of Ultra-precision Machining Technology, Department of Industrial and Systems Engineering, The Hong Kong Polytechnic University, Hung Hom, Kowloon, Hong Kong, China.

Corresponding Author / Email: canbin.zhang@connect.polyu.hk, TEL: +85-256-23-2030

2 son-x Gmbh, Aachen, Germany

#

KEYWORDS: Ultra-precision machining, difficult-to-machine materials, Ultrasonic vibration-assisted sculpturing, microlens array, feature size

Ultrasonic vibration-assisted cutting (UVAC) is a technically feasible way to fabricate 3D microstructures on steel mould for producing optical components by mass production. To fabricate microlens arrays with small feature sizes on steel workpiece, ultrasonic vibration-assisted sculpturing (UVAS) was used and the effects of feature sizes of microlens array were investigated. Circular target lines were machined under various conditions in order to optimize machining parameters. Moreover, theoretical form errors were determined to evaluate the technical feasibility of UVAS of microlens arrays with various feature size. Hence, the optimized machining parameters were used to cut microlens arrays with 0.1 mm lenslet radius. The results showed that UVAS by one cut is feasible in fabrication of microlens array with micro feature sizes. However, with the decrease of feature size, material recovery, burr generation and plastic defects became prominent and resulted in poor machining quality.

NOMENCLATURE

r = lenslet radius
d = lenslet depth
p = lenslet pitch

1. Introduction

In many advanced optical systems and products, the need for micro-structured functional surfaces has been rising, including diffraction gratings, microlens arrays, pyramid arrays, and retroreflective arrays has been rising [1]. Moreover, high-temperature forming process is an efficient way to enhance their widespread applications. Making moulds out of difficult-to-machine materials like hardened steel is very important. UVAC is recognized as a feasible technology with less tool wear [2] and better surface finish [3] due to intermittent cutting characteristics.

In the author's previous study, UVAS has been applied to fabricate microlens arrays with various edge shapes [4], taking into no account of the size effect. In this study, the effects of feature size were investigated. Circular target lines with different lenslet radii were machined under various parameters to study their effects on form error, including nominal cutting speed, depth-of-cut and tool clearance angle. Besides, theoretical form error was calculated to evaluate machining accuracy of UVAS of microlens arrays with various feature sizes. Hence, a microlens array with a lenslet radius of 0.1 mm was machined for form accuracy and surface quality analysis.

2. Size effects in HFUVAS of microlens array

2.1 Theoretical form error caused by constant tool nose in UVAS of microlens array

In UVAS of microlens array, a round tool with a constant nose radius (R_t) moves along the target profile of a lenslet, whose curvature radius increases to the largest at the lowest point ($r = R_t$) and then decreases. As a result, there exists a form deviation between the theoretical and experimental lens array as shown in Fig. 1. The largest deviation appears at sharp peaks, where represent the form error of the

whole surface. Fig. 2 summarizes the theoretical form error with regard to lenslet depth for various lenslet radii. For a constant lenslet radius, the theoretical from error increase with increasing lenslet depth. When the lenslet radius decreases from 1.0 mm to 0.1 mm, the theoretical from error increase slowly, but significantly at $r = 0.1$ mm. Therefore, to fabricate a microlens array with a small feature size, the lenslet depth must be appropriately selected to avoid an intolerant form error.

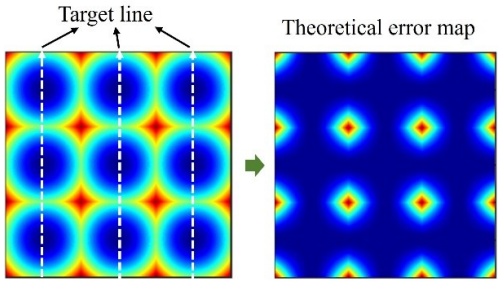

Fig. 1 Form deviation between theoretical and experimental microlens array.

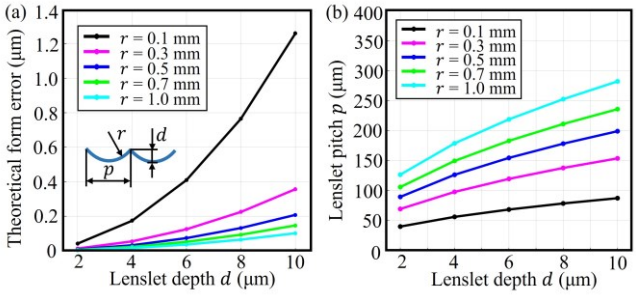

Fig. 2 Relationships between: (a) theoretical form error and lenslet depth, (b) lenslet pitch and lenslet depth, with various lenslet radii.

2.2 Form error induced by material recovery in UVAS of circular target line

Fig. 3 presents the stress zone along the target line of the microlens array. In the horizontal cutting stage as shown in Fig. 3 (a), the material in advance of the cutting tool separated at point A and the lower part flows along the tool edge and then recovers after unloading. In this process, workpiece experiences deformation at the contact point B with a vertical displacement of h_s apart from the contact depth h_c, which leads to a total penetration depth of s, namely spring back. In the downward cutting stage as shown in Fig. 3 (b), the effective clearance angle is reduced. Especially when the maximum slope angle is close to the tool clearance angle with small feature size, the contact point is transferred from B to B′ to maintain a comparable value of h_c for material flow. As a result, the stress zone is enlarged with a larger thrust force and with an increased h_s, thereby resulting in increased spring back s. This phenomenon was termed as the indentation effect [5]. In contrast, in the upward cutting stage, the effective clearance angle is increased so the stress zone and spring back are reduced. As a result, it can be concluded that material recovery decreases gradually along one lenslet. Fig. 3(d) shows that the maximum slope angle of the target line increases with decreasing lenslet radius, leading to larger material recovery.

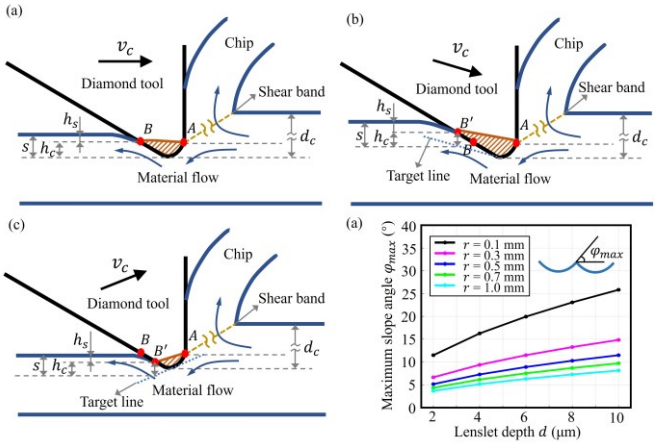

Fig. 3 Schematics of stress zone along (a) horizontal, (b) downhill, (c) uphill target line, (d) relationship between maximum slope angle and lenslet depth of the target line.

3. Experimental parameters and setups

A circular target line is determined by Eq. (1):

$$z(y) = \mathrm{r} - \sqrt{r^2 - [y - p(i - 0.5)]^2} - d \qquad (1)$$

where i denotes the sequence number of a lenslet along the y direction. r, d and p are the lenslet radius, lenslet depth and lenslet pitch of the target line. Table 1 shows the experimental parameters of the four groups. In each group, the nominal cutting speed was set as 25, 50, 100, 200 mm/min. In group 1 and group 2, two target lines were cut. For target line 1, d, r and p were set as 5, 1000 and 200 μm, with a maximal slope angle of 5.7 °. For target line 2, d, r and p were set as 5, 205 and 90 μm, with a maximal slope angle of 12.7 °. In group 2 and 3, the structures were machined by layers with depths-of-cut of 3, 2, 1 μm and 1, 1, 1, 1, 1, 1 μm, respectively. Furthermore, in group 2 and group 4, diamond tools with clearance angles of 15 ° and 20 ° was used to cut the structures. Diamond tools had a rake angle of 0 ° and nose radius of 1 mm. In each depth-of-cut, the tool path was segmented into two steps to avoid movement error caused by quick acceleration at sharp edges, as presented in Fig. 4.

Table 1 Experimental parameters of the cutting experiment

Machining parameters	Group1	Group2	Group3	Group4
Cutting speed	25, 50, 100, 200 mm/min			
Target line	Line 1	Line 2		
Workpiece material	Mirrax 40 steel			
Tool clearance angle	15°			20°
Depth-of-cut (μm)	3-2-1	3-2-1	1	3-2-1
Lubricant	Clairsol 330/odourless kerosene, MQL			

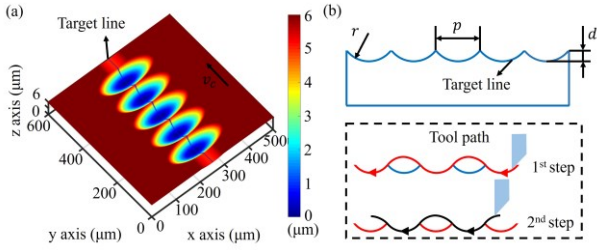

Fig. 4 (a) Modelling of target line and the generated structure, (b) tool path generation of the target line.

Fig. 5 presents the experimental setups. An ultrasonic vibration system (UTS2) was configurated on Moore Nanotech 350 FG. In the experiment, UTS2 had an operation frequency of 104 kHz and the input current was 30 mA, having a vibration amplitude of about 1.0 μm in the cutting direction. A Zygo white interferometer was used to evaluate surface accuracy and roughness of the 3D microstructures.

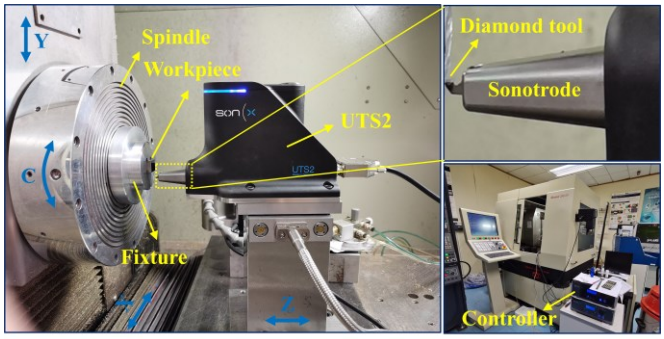

Fig. 5 Photography of experimental setups.

4. Results and discussions

4.1 HFUVAS of circular target line with various parameters

Fig. 6 presents the method for form accuracy analysis. The surface topography of the machined 3D microstructures were measured to obtain cut line, namely AB. Two lowest points of the lenslets were identified and used as the reference points (RP) to match with those of the target line and then to obtain the form error.

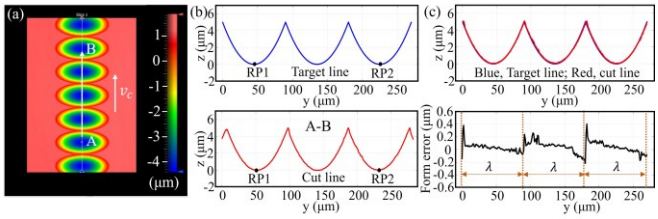

Fig. 6 Method for form accuracy analysis, (a) measured 3D topography, (b) the target line and cut line, (c) matching result and form error.

Fig. 7 shows the form error of Group 1. Target line 1 has a larger lenslet pitch with a smaller maximal slope angle, resulting in a small form error for all the selected nominal cutting speeds. The form error of group2 was larger with a higher maximal slope angle of target line 2, which exhibited an increasing trend with increasing nominal cutting speed, especially at 200 mm/min where the total form error reached more than 1 μm. The first and the third lenslet were cut by the 1st setup while the second lenslet was cut by the 2nd step. A sharp increase of form error appeared at the entrance of the first and the third lenslet, which could be caused by burr generation happening on the 2nd step due to discontinuous machining. Apart from such a sharp increase, the form error of one lenslets shew a decreasing trend, meaning that the material on the downward target line was less cut. This is due to more elastic recovery caused by a small effective clearance angle due to the indentation effect as discussed in section 2.2.

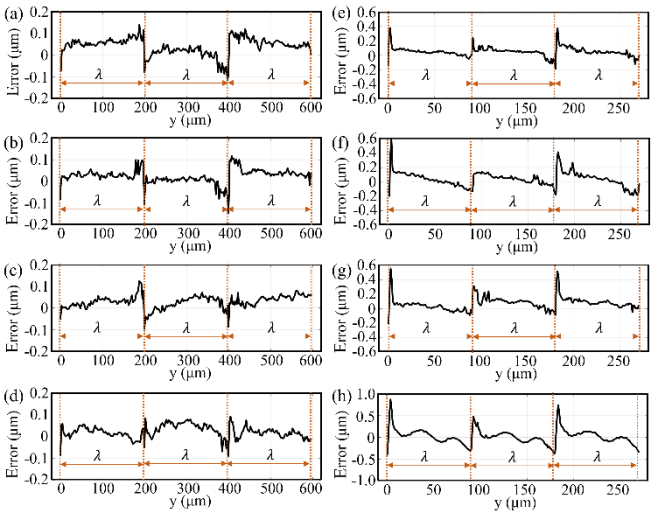

Fig. 7 Form error of group1: (a) 25 mm/min, (b) 50 mm/min, (c) 100 mm/min, (d) 200 mm/min; form error of group2: (e) 25 mm/min, (f) 50 mm/min, (g) 100 mm/min, (h) 200 mm/min.

Comparing Fig. 8(a)-(d) with Fig. 7(e)-(h), it can be found that form errors of all nominal cutting speeds with depths-of-cut of 3-2-1 μm was comparable to the results of depths-of-cut of 1-1-1-1-1-1 μm, indicating that depth-of-cut put a limited effect on from error in HFUVAS. By comparison between Fig. 8(e)-(h) and Fig. 7(e)-(h), the form errors with the clearance angle of 20° were significantly reduced and they were less than 0.5 μm except for the condition of 200 mm/min. Based on these results, the effects of machining parameters were identified and the optimized machining parameters to reduce form error would be: an appropriate tool clearance angle to maintain a suitable effective clearance angle, 100 mm/min in nominal cutting speed, depth-of-cut is expected to be gradually reduced to improve machining efficiency. Fig. 9 presents the surface roughness of one lenslet in group4, with an arithmetic roughness Sa of about 10 nm.

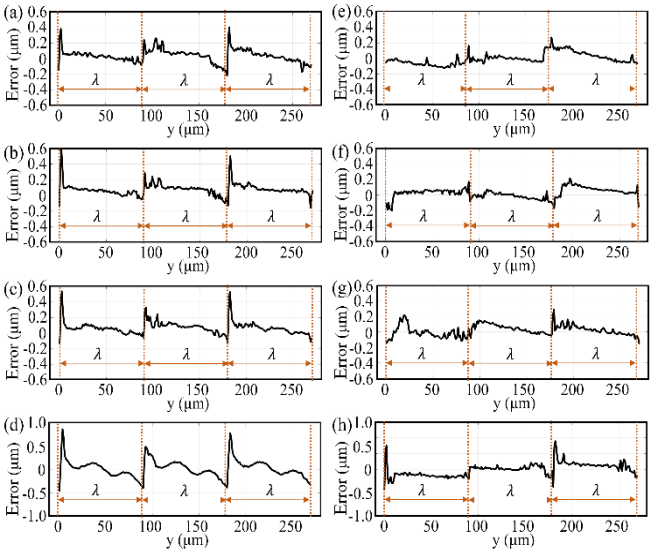

Fig. 8 Form error of group3: (a) 25 mm/min, (b) 50 mm/min, (c) 100 mm/min, (d) 200 mm/min; form error of group4: (e) 25 mm/min, (f) 50 mm/min, (g) 100 mm/min, (h) 200 mm/min.

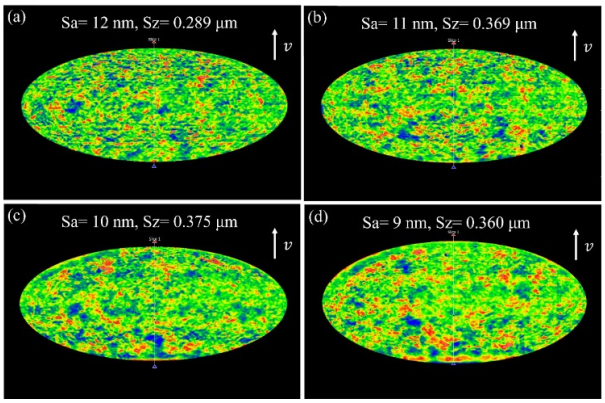

Fig. 9 Surface roughness of one lenslet of group4: (a) 25 mm/min, (b) 50 mm/min, (c) 100 mm/min, (d) 200 mm/min.

4.2 UVAS of microlens array with small feature size

To study machining performance of UVAS of microlens array with small feature size, a microlens array with r of 100 μm and d of 2.5 μm was machined with 100 mm/min cutting speed, 3, 2, 1 μm depth-of-cut, 20° tool clearance angle. As shown in Fig. 10, the line error was about 0.5 μm in the cutting direction, and the error near sharp edges took a large part, which was larger than the result in Fig. 8(g). Besides, cut line and target line along the feed direction had a great deviation as compared with the result of larger feature size [4], which has a high possibility to be caused by material recovery. These imply that with the decrease of feature size, ploughing behavior and burr generation become more significant, leading to difficulties in accurate material removal.

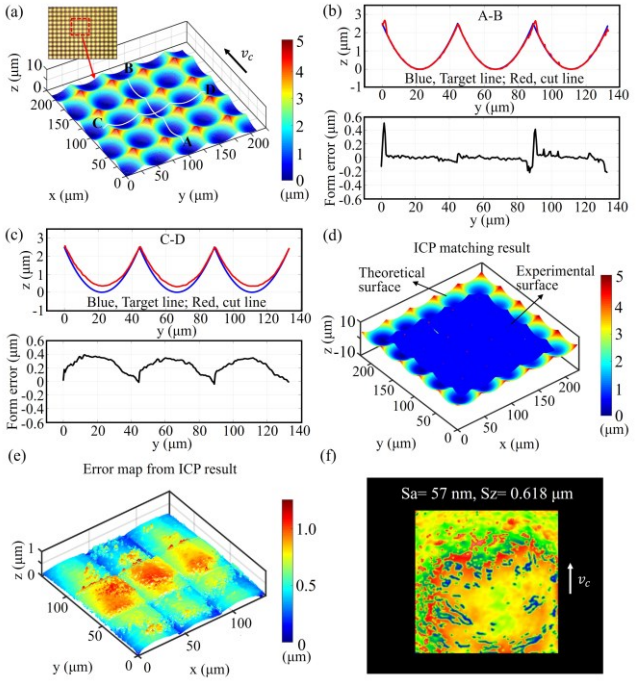

Fig. 10 Machining quality of microlens array: (a) measured 3D topography, (b) line analysis of AB, (c) line analysis of CD, (d) matching of theoretical and experimental surfaces, (e) error map from matching result, (f) one lenslet's surface morphology and roughness.

The theoretical and experimental microstructures were matched with each other by iterative closest point (ICP) matching. The matching result and error map were identified as shown in Fig. 10(d) and (e), having a form error more than 1 μm. Sharp-edge burrs and surface defects were the main reasons for the total form error. The surface quality of lenslet was poor, accompanied by plenty of plastic deformation and surface smearing, which were the evidence of ploughing behavior.

5. Conclusions

This study investigates the size effects in HFUVAS of microlens array. Some findings are given as follows:

1. Form error increased with decreasing feature size due to material recovery and burr generation in HFUVAS of circular target line. An appropriate selection of tool clearance angle, nominal cutting speed and depth-of-cut is contributed to improve machining efficiency.

2. Theoretical form error increased with decreasing feature size in UVAS of microlens array by constant tool nose. Besieds, sharp-edge burrs generation and surface plastic defects due to ploughing behavior became intense due to a small feature size.

ACKNOWLEDGEMENT

The authors would like to show the gratitude to the financial support from the Research Office (Project code: RK2Z) from The Hong Kong Polytechnic University, and the contract research project between the state key laboratory of ultra-precision machining technology of The Hong Kong Polytechnic University and Son-X, Gmbh, Aachen, Germany.

REFERENCES

1. Zhang, S., Zhou, Y., Zhang, H., Xiong, Z., & To, S., "Advances in ultra-precision machining of micro-structured functional surfaces and their typical applications," Int. J. Mach. Tools Manuf., Vol. 142, pp. 16-41, 2019.

2. Shamoto, E., & Moriwaki, T., "Ultaprecision diamond cutting of hardened steel by applying elliptical vibration cutting," CIRP Ann-Manuf. Technol., Vol. 48, No. 1, pp. 441-444, 1999.

3. Zhang, X., Kumar, A. S., Rahman, M., Nath, C., & Liu, K., "Experimental study on ultrasonic elliptical vibration cutting of hardened steel using PCD tools," J. Mater. Process. Technol., Vol. 211, No. 11, pp. 1701-1709, 2011.

4. Zhang, C., Cheung, C. F., Liang, X., & Bulla, B., "High-frequency ultrasonic vibration-assisted sculpturing with a smoothed tool path for optical 3D micro-structured surfaces with sharp edges," J. Manuf. Process., Vol. 101, pp. 1246-1256, 2023.

5. Yuan, W., & Cheung, C. F., "Theoretical and experimental investigation of the tool indentation effect in ultra-precision tool-servo-based diamond cutting of optical microstructured surfaces," Opt. Express, Vol. 29, No. 24, pp. 39284-39303, 2021.